Parallel-Coupled Line Filters With Enhanced Stopband Performances

Wael M. Fathelbab, *Senior Member, IEEE,* and Michael B. Steer, *Fellow, IEEE*

***Abstract*—A new class of parallel-coupled line filters with broad stopband response is introduced. The design is based on the synthesis of bandpass prototypes with pre-defined upper stopband characteristics. The new filters have uniform- and stepped-impedance resonators, some of which are loaded by open-circuited stubs at their open-circuited ends. A seventh-order filter implementation is presented with a fundamental passband centered at 1 GHz. The measured wide-band transmission characteristic of the filter demonstrated a broad upper stopband and was in agreement with simulations. The performance of the new filter is also compared with the characteristic of a conventionally designed filter to highlight the advantages of the proposed design method.**

***Index Terms*—Capacitively loaded resonators, high-pass/bandpass filter prototypes, parallel-coupled line (PCL) filters, spurious stopband rejection, uniform/stepped-impedance resonators.**

I. Introduction

PARALLEL-COUPLED line (PCL) filters [1] do not require ground connections and, thus, are easily fabricated in planar form. They have traditionally been used to realize passband bandwidth ratios ranging from as small as $1.02:1$ to as large as $3:1$ [2]. Another advantage of PCL filters is that their resonators can be folded into hairpin form, making them suitable for applications with space restrictions [18], [19]. However, when this class of filters is realized on an inhomogeneous media such as microstrip or coplanar waveguide, it suffers from poor upper stopband performance and typically has spurious passbands centered at harmonics of the fundamental passband center frequency, f_o.

Considerable efforts to improve the stopband performance of microstrip PCL filters have been directed at suppressing the harmonic spurious passband located at $2f_o$. This was done by compensating for the difference between the even- and odd-mode phase velocities of the inhomogeneous media in a variety of ways. In one approach, the coupled lines were loaded by lumped capacitors [3] or meandered [4]. Other approaches introduced ground-plane apertures underneath the coupled lines [5]–[7] or utilized suspended substrates with dielectric overlay [8], [9]. Other attempts to suppress the undesired spurious passbands introduced geometrical perturbations to the uniform-impedance resonators in the coupling regions [10]–[14], loaded them by split-ring resonators [15], or alternatively utilized stepped-impedance resonators [16]. More recently, a PCL filter with uniform-impedance resonators loaded by open-circuited stubs at all its open-circuited ends demonstrated suppression of the second- and third-ordered harmonic passbands [17]. However, the design approach presented requires generalization.

This paper presents a circuit-oriented design approach for PCL filters based on classical network synthesis techniques. The advantages of this approach are primarily design insight and exploitation of all parameters of a transfer function leading to optimum network topologies. The new PCL filters are derived from synthesized bandpass prototypes with controlled upper stopband responses. This is done by systematic application of appropriate circuit transformations on the initial bandpass prototype resulting in a class of PCL filters comprising uniform- and stepped-impedance resonators some of which are loaded by open-circuited stubs at their open-circuited ends.

This paper begins with an outline in Section II of the traditional design procedure for PCL filters using uniform- and stepped-impedance resonators. The new design method is then presented in Section III. In Section IV, a bandpass filter prototype is synthesized and appropriately transformed to a realizable PCL filter. Finally, in Section V, the measured characteristic of the new filter is contrasted to the measured performance of a PCL filter utilizing optimized stepped-impedance resonators.

II. Review of the Design of Uniform- and Stepped-Impedance PCL Filters

The traditional design of PCL filters is based on the S-plane high-pass prototype depicted in Fig. 1(a) with S being the Richards variable defined as

$$S = j\Omega_{\mathrm{HP}} = j\tan(\theta_{\mathrm{HP}}) = j\tan\left(\frac{\pi}{2}\frac{f}{f_o}\right). \qquad (1)$$

In (1), f and S are the real and complex frequency variables, respectively, and f_o is the center frequency of the fundamental passband in the f-plane. This prototype can be synthesized in the S-plane by exact methods [22], [25] and then transformed to the f-plane using (1). The rectangular blocks in the S-plane prototype of Fig. 1(a) are known as unit elements (U.E.s) [25] and become transmission lines in the f-plane, whereas the capacitors represent open-circuited stubs in the f-plane. The distributed elements in the f-plane are all quarter-wave-length long at f_o. Now each building block in the S-plane prototype comprises a pair of series capacitors separated by a U.E., and this can be replaced by a PCL section using the equivalence shown in Fig. 1(b). The critical property of the transition from the S-plane to the corresponding f-plane is that the f-plane response of

Manuscript received June 9, 2005. This work was supported by the U.S. Army Research Office as a Multi-disciplinary University Research Initiative on Multi-functional Adaptive Radio Radar and Sensors under Grant DAAD19-01-1-0496.

The authors are with the Department of Electrical and Computer Engineering, North Carolina State University, Raleigh, NC 27695-7911 USA (e-mail: wmfathel@ncsu.edu).

Digital Object Identifier 10.1109/TMTT.2005.859871

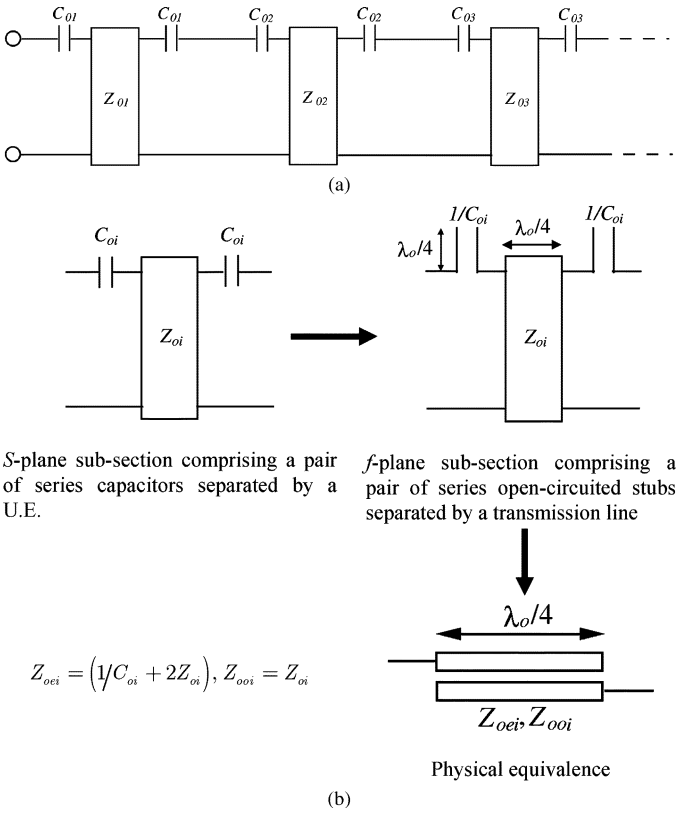

Fig. 1. (a) S-plane high-pass prototype. (b) Subsection equivalence.

the prototype becomes a periodic bandpass function with spurious passbands centered at odd multiples of f_o. This is an intrinsic property of the prototype of Fig. 1(a). An additional complexity arises when this filter is realized on an inhomogeneous transmission media due to the inequality between the even- and odd-mode phase velocities. This effect can be investigated by utilizing the full $ABCD$ matrix (see the Appendix) of each PCL section in a filter for a known even- to odd-mode velocity ratio. It can be shown that the effect of the inhomogeneous media creates additional spurious passbands centered approximately at even multiples of f_o [3]–[16].

To some extent it is possible to alter the positions of the spurious passbands of conventional PCL filters by using stepped-impedance resonators. An excellent account of this technique presenting useful design equations can be found in [16]. Fig. 2(a) shows a Type 1 stepped-impedance resonator where $Z_s > Z_r$ [16]. The design approach using Type 1 resonators is briefly explained as follows. The uniform resonators of each PCL section in a conventional filter [see Fig. 1(b)] are staggered by a defined amount. This effect is consequently compensated for by setting the characteristic impedances of the uncoupled line sections of the resonators to a fixed high value Z_s. Consequently, the length l_s of each uncoupled line in the filter is then optimized until the return loss of the fundamental passband is restored. A pair of stepped-impedance resonators is shown in Fig. 2(b). Intuitively one could conclude that a change in the stopband performance of a filter will depend on the amount of stagger and the impedance ratio Z_s/Z_r. Now the effect of the inhomogeneous media can be investigated as discussed above. This process could be iterated on until

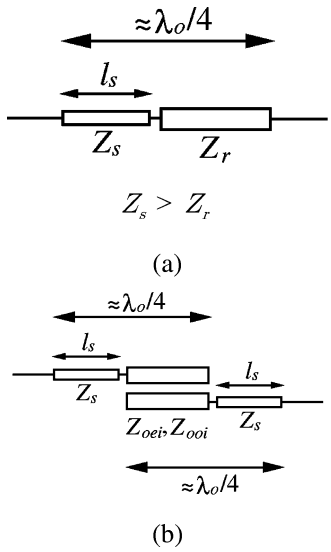

Fig. 2. (a) Type 1 stepped-impedance resonator from [16]. (b) Pair of coupled stepped-impedance resonators.

a suitable stopband performance is reached. In general, this technique offers limited stopband improvement and is best suited to applications where a small shift in the spurious passbands would block harmonics of the input signal from passing through the filter. Thus, the spurious passbands of a filter are not eliminated, but in effect, the stopband characteristic is altered to suit a particular specification [16]. There is also a Type 2 stepped-impedance resonator with $Z_s < Z_r$ resulting in filters with slightly different stopband behavior to those utilizing Type 1 resonators [16]. In the following, we investigate how the design of PCL filters based on S-plane bandpass prototypes would lead to better stopband performances.

III. Design of New PCL Filters

The prototype proposed here is shown in Fig. 3(a). It is classified as an S-plane bandpass prototype with the Richards variable redefined as

$$S = j\Omega_{\mathrm{BP}} = j\tan(\theta_{\mathrm{BP}}) = j\tan\left(\frac{\pi}{2}\frac{f}{f_r}\right). \qquad (2)$$

In (2), f and S are as defined previously, but now f_r is the center frequency of the first upper stopband in the f-plane. Similar to the S-plane high-pass prototype discussed in Section II, this prototype can be synthesized in the S-plane by exact methods [23]–[25] and then transformed to the f-plane using (2). In the f-plane, the U.E.s, capacitors, and inductors of Fig. 3(a) become transmission lines and open- and short-circuited stubs, respectively, and are all a quarter-wave-length long at f_r. It has been shown in [26] that the f-plane response of an S-plane bandpass prototype is periodic with a fundamental passband centered at $f_o (f_o < f_r)$ and spurious passbands centered at

$$i \cdot 2f_r - f_o \text{ and } i \cdot 2f_r + f_o, \qquad i = 1, 2, 3 \ldots. \qquad (3)$$

Thus, synthesis based on an S-plane bandpass prototype has great flexibility in controlling the location of the first pair of spurious passbands in the f-plane. This is possible by selecting a large commensurate frequency f_r to shift the upper spurious

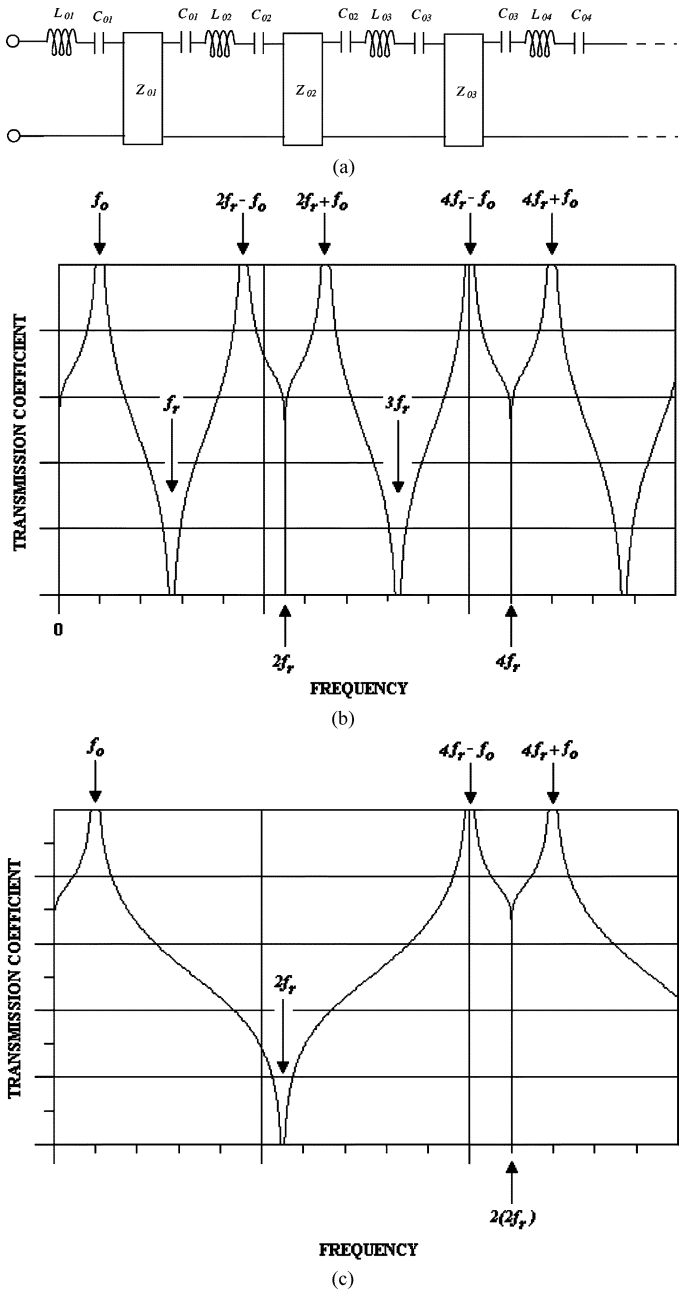

Fig. 3. (a) S-plane bandpass prototype. (b) Real frequency response for one commensurate frequency f_r. (c) Response after doubling f_r.

passbands further away from the fundamental passband. Essentially this is the design rationale of the new PCL filters, which closely resembles the design of conventional bandpass filters such as combline [20], [21], [24], [25].

A typical f-plane response of the proposed prototype is depicted in Fig. 3(b) where it is seen that the series S-plane LC sections (i.e., f-plane short- and open-circuited stubs) contribute to multiple transmission zeros at $i \cdot f_r$ where $i = 1, 2, 3 \ldots$. By doubling the commensurate frequency (i.e., moving from f_r to $2f_r$) leads to the response shown in Fig. 3(c) where the spurious responses are shifted leaving behind a broad stopband region.

Now we focus our attention on the circuit structure of Fig. 3(a). Through a number of circuit transformations we convert this into a form that can be implemented using distributed

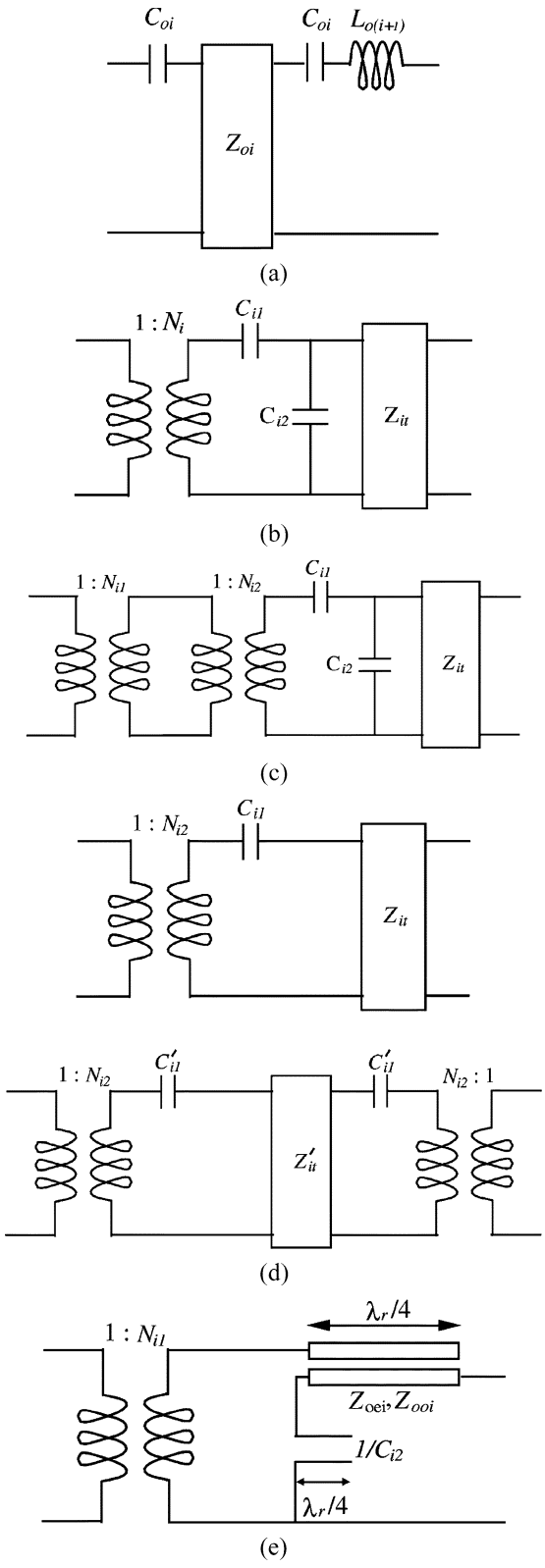

Fig. 4. Exact circuit transformations. (a) Basic S-plane sub-circuit. (b) Application of relevant Kuroda transformations. (c) Splitting of the $1 : N_i$ transformer. (d) Distribution of the series capacitor. (e) f-plane subsection comprising a PCL loaded by an open-circuited stub at the left open-circuited end.

elements. Consider the S-plane sub-circuit shown in Fig. 4(a) comprising a U.E. separating a pair of series capacitors fol-

lowed by a series inductor. It is feasible to transform the series *LC* section across the U.E. by using relevant Kuroda transformations [25], [26]. This leads to the sub-circuit of Fig. 4(b), whose element values are related to those of Fig. 4(a) through the following relations:

$$\begin{aligned} N_i &= 1 + \frac{1}{Z_{oi}C_{oi}} \\ C_{i1} &= \frac{C_{oi}}{N_i(N_i-1)C_{oi}Z_{oi} + N_i^2} \\ C_{i2} &= \frac{L_{o(i+1)}}{N_i Z_{oi}\left(N_i Z_{oi} + L_{o(i+1)}\right)} \\ Z_{it} &= N_i Z_{oi} + L_{o(i+1)}. \end{aligned} \tag{4}$$

Now the series capacitor C_{i1} and the U.E. of characteristic impedance Z_{it} form a single PCL section if a $1:N_{i2}$ transformer is extracted from the existing $1:N_i$ transformer. The value of this transformer is

$$N_{i2} = \frac{1}{\sqrt{\dfrac{Z_{it}}{Z_{it} + \dfrac{1}{C_{i1}}}}} \tag{5}$$

leaving a $1:N_{i1}$ transformer of turns ratio

$$N_{i1} = \frac{N_i}{N_{i2}}. \tag{6}$$

This step leads to Fig. 4(c). The $1:N_{i2}$ transformer together with the series capacitor and U.E. is the S-plane model of an open-circuited coupled-line section in homogenous media [25]. Thus, let us for a while ignore the shunt capacitor C_{i2} and just investigate the sub-circuit of Fig. 4(d). If a relevant Kuroda transformation is applied to spread the series capacitor C_{i1}, then the following relations:

$$\begin{aligned} C'_{i1} &= \frac{1}{N_{i2}(N_{i2}-1)Z_{it}} \\ Z'_{it} &= N_{i2}Z_{it} \end{aligned} \tag{7}$$

hold for the circuits of Fig. 4(d). Hence, the modal impedances of the PCL section loaded by an open-circuited stub (of characteristic impedance $1/C_{i2}$) at the left open-circuited end are then evaluated [26] using (7) to give

$$Z_{oei} = \frac{\left(\dfrac{1}{C_{i1}}' + 2Z'_{it}\right)}{N_{i2}^2} \quad Z_{ooi} = \frac{\left(\dfrac{1}{C'_{i1}}\right)}{N_{i2}^2}. \tag{8}$$

This concludes the transformation of the subsection of Fig. 4(a) into that of Fig. 4(e).

Fig. 5(a) shows an S-plane bandpass prototype where the sub-circuits enclosed in the dashed boxes can be systematically transformed as just described. The transformation results in the f-plane filter shown in Fig. 5(b). This is only one among many that could be transformed using the new method. In practical terms, it might be desirable not to transform all the inductors across the U.E.s to form PCLs loaded by open-circuited stubs. This is typically due to extreme element values that might lead to realization difficulties on a printed circuit board (PCB).

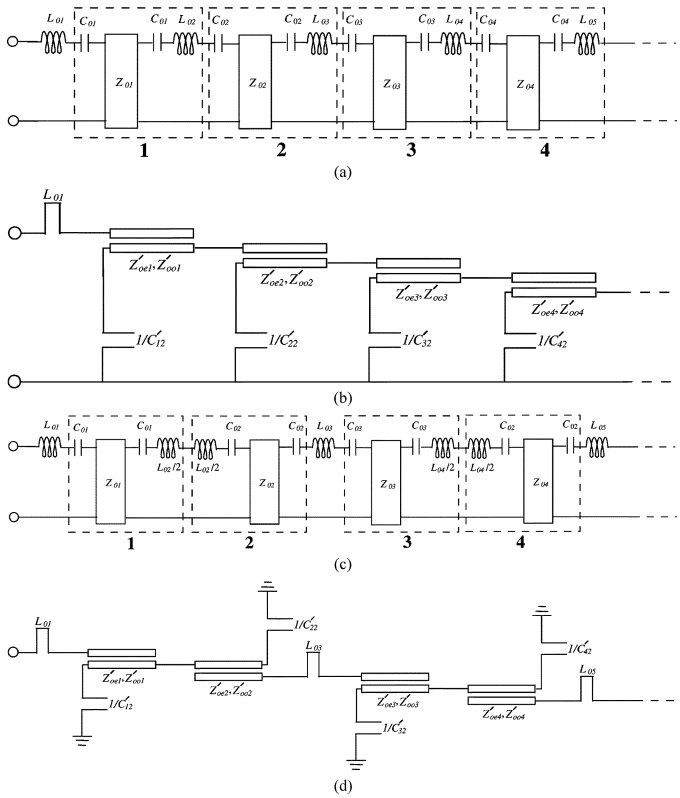

Fig. 5. (a) S-plane bandpass prototype and (b) its corresponding f-plane filter comprising PCLs loaded by open-circuited stubs at the left open-circuited ends. (c) An S-plane bandpass prototype; and (d) its corresponding f-plane filter comprising PCLs loaded by open-circuited stubs at either the left- or the right-hand-side open-circuited ends. The resulting filters are derived after application of the circuit transformation scheme described in Fig. 4 on the sub-circuits enclosed in the dashed boxes of the S-plane prototypes.

To a great extent these constraints can be resolved dependent on how the initial S-plane bandpass prototype is transformed. For this reason, let us apply the transformation steps to the subsections (enclosed in the dashed boxes) of the S-plane prototype shown in Fig. 5(c). This prototype is identical to that of Fig. 5(a), except that some of the inductors are now divided into pairs. Upon transformation, the f-plane filter illustrated in Fig. 5(d) results. As seen from Fig. 5(d), the filter inevitably has some series short-circuited stubs in its main signal path. We propose approximating these stubs by sections of high-impedance transmission lines as follows.

A section of transmission line of short electrical length at f_o and of high characteristic impedance Z_o has an input impedance approximately equal to

$$Z_{\text{in}} \simeq j(Z_o)(\theta') = j(Z_o)\left(\frac{\pi}{2}\frac{f_o}{f'_r}\right). \tag{9}$$

where f'_r is the quarter-wave-length frequency of the transmission line. On the other hand, a series short-circuited stub of characteristic impedance L is resonant at f_r and has an input impedance at the center of the fundamental passband equal to

$$Z_{\text{in}} = j(L)\tan(\theta_{\text{BP}}) = j(L)\tan\left(\frac{\pi}{2}\frac{f_o}{f_r}\right). \tag{10}$$

The above equations are approximately equal for passband bandwidths up to an octave (i.e., $2:1$ bandwidth ratio) and,

hence, can be simultaneously solved for the resonant frequency of the transmission line to give

$$f_r' = \frac{\pi}{2}\frac{Z_o f_o}{L\tan\left(\frac{\pi}{2}\frac{f_o}{f_r}\right)}. \tag{11}$$

Subsequently the physical length of the transmission line can be evaluated for a given substrate specification. In general, the higher the line impedance that can be realized, the better the approximation. However, over half of the total number of S-plane inductors in a prototype is transformed into open-circuited stubs and, thus, the shape of the f-plane transfer function of a prototype in the stopband region is maintained after the above approximation. This completes the filter design approach.

IV. Experimental PCL Filter

Design of a filter is best illustrated using an example following the common approach in filter papers. The outline specification is to obtain a bandpass filter at 1 GHz with a broad stopband response. A seventh-order approximation function was first developed in the S-plane [23]–[25]. In the f-plane, the response has a fundamental passband center frequency f_o of 1 GHz and a commensurate frequency f_r of 2.75 GHz, which according to (3), leads to the existence of a first pair of spurious passbands centered at 4.5 and 6.5 GHz. The return loss of the fundamental passband was 16 dB and its bandwidth ratio was $1.22:1$ (i.e., 20%) leading to lower and upper band-edge frequencies of 0.9 and 1.1 GHz, respectively. Following standard synthesis, a physically symmetrical S-plane network results and, thus, only half of it is shown in Fig. 6(a).

We shall now examine the inter-resonator couplings after transforming all the inductors in the prototype into open-circuited stubs to yield a PCL filter similar in topology to that of Fig. 5(b). The objective here is twofold: firstly, to numerically demonstrate the circuit transformation process discussed in Section III, but secondly, to see how the element values of the resulting filter are distributed. From the first box [of the prototype of Fig. 6(a)], we have the following parameters:

$$C_{o1} = \frac{1}{119.025} \quad Z_{o1} = 34.52 \quad L_{o2} = 713.332 \tag{12}$$

corresponding to a subsection such as that of Fig. 4(a). Now, according to the relations of (4), a set of element values are evaluated to give

$$\begin{aligned} N_1 &= 4.448 \\ C_{11} &= \frac{1}{2884.297} \\ C_{12} &= \frac{1}{186.595} \\ Z_{1t} &= 866.876. \end{aligned} \tag{13}$$

This transforms the subsection to that of Fig. 4(b). A $1:N_{12}$ transformer is then extracted from the $1:N_1$ transformer using (5). The value of the turns ratio of this transformer is

$$N_{12} = 2.08 \tag{14}$$

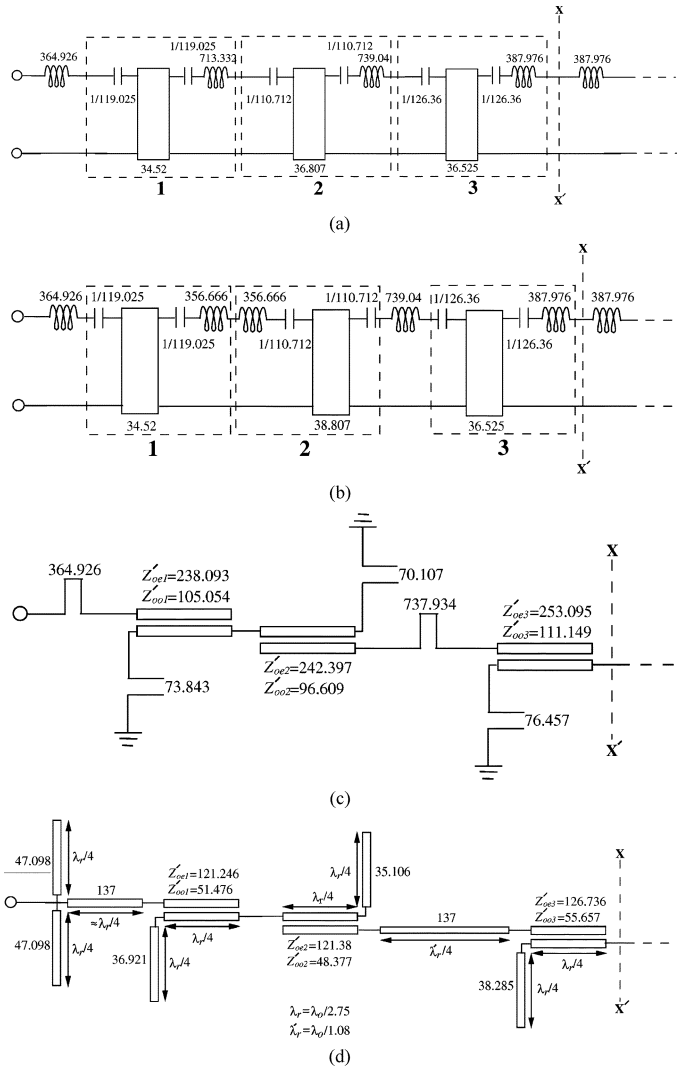

Fig. 6. Development of a seventh-order PCL filter. (a) Synthesized S-plane prototype in a 50-Ω system. (b) After splitting some of the inner inductors into pairs. (c) Topology of the f-plane filter depicting inter-resonator couplings. (d) Filter's electrical layout. (The $X - X'$ is the plane of symmetry.)

which, according to (6), leaves a $1:N_{11}$ transformer of turns ratio

$$N_{11} = 2.138. \tag{15}$$

This takes us to a sub-circuit of similar topology to that of Fig. 4(c). The next step is to evaluate the element values of the sub-circuit of Fig. 4(d) using (7) to give

$$C_{11}' = \frac{1}{1947.35} \quad Z_{1t}' = 1803.102. \tag{16}$$

Now, according to (8), the modal impedances of the first pair of PCLs loaded by an open-circuited stub of characteristic impedance $1/C_{12} = 186.595\ \Omega$ at the left—hand-side open-circuited end are calculated as

$$Z_{oe1} = 1283.643\,\Omega \quad Z_{oo1} = 450.108\,\Omega. \tag{17}$$

This concludes the transformation of the first subsection to a topology similar to that of Fig. 4(e). In a similar fashion, the

sub-circuits enclosed in the second and third boxes are also transformed leading to the following element values:

$$\begin{aligned} N_{21} &= 2.14 \\ \frac{1}{C_{22}} &= 176.964\ \Omega \\ Z_{oe2} &= 1351.136\ \Omega \\ Z_{oo2} &= 403.706\ \Omega \end{aligned} \tag{18}$$

and

$$\begin{aligned} N_{31} &= 1.737 \\ \frac{1}{C_{32}} &= 231.266\ \Omega \\ Z_{oe3} &= 765.535\ \Omega \\ Z_{oo3} &= 336.182\ \Omega. \end{aligned} \tag{19}$$

It must be appreciated that each transformed subsection has a $1 : N_{i1}$ transformer associated with it. Each of these transformers is eliminated by scaling down the modal impedances of the PCL sections together with the characteristic impedances of the stubs in the filter. This step leads to a symmetrical f-plane filter compatible with that of Fig. 5(b) having the following element values:

$$\begin{aligned} L_{o1} &= 364.926\ \Omega \\ Z'_{oe1} &= 280.749\ \Omega \\ Z'_{oo1} &= 98.454\ \Omega \\ \frac{1}{C'_{12}} &= 40.805\ \Omega \\ Z'_{oe2} &= 64.922\ \Omega \\ Z'_{oo2} &= 19.72\ \Omega \\ \frac{1}{C'_{22}} &= 8.442\ \Omega \\ Z'_{oe3} &= 12.093\ \Omega \\ Z'_{oo3} &= 5.31\Omega \\ \frac{1}{C'_{32}} &= 3.653\ \Omega. \end{aligned} \tag{20}$$

It is desired to construct the filter on an FR4 board with a substrate thickness of 62 mil (1.57 mm), relative dielectric constant of 4.7, and loss tangent of 0.016. Practical constraints imposed by the PCB manufacturer are that any track width and spacing between tracks must not exceed a minimum of 7 mil (0.177 mm). From (20), the coupling coefficients of the PCLs were calculated and the *LinCal* sub-routine of Agilent's Advanced Design System (ADS)[1] was utilized to obtain a rough estimate of physical dimensions. Unfortunately, the resulting dimensions were unrealizable on this type of board and, also as seen from (20), some of the impedances of the stubs are low. Therefore, transformation of the initial prototype to the proposed network topology of Fig. 5(d) was done. The steps involved are shown in Figs. 6(b) and (c). It can now be seen from the circuit of Fig. 6(c) that the modal impedances are actually high and would still be unrealizable on our PCB. Scaling down the impedance matrix representing this circuit is, therefore, necessary at this point. This step changed the system impedance of the filter from 50 to 50/2.5 Ω and imposes the placement of an impedance inverter of value 31.62 Ω at each port of the filter. Each inverter is then approximated by a transmission line and the scaled series short-circuited stubs [near the filter ports, see Fig. 6(c)] of characteristic impedance (364.926/2.5) Ω are subsequently transformed into open-circuited stubs using a Kuroda transformation.

[1]ADS, ver. 2003A, Agilent Technol., Palo Alto, CA.

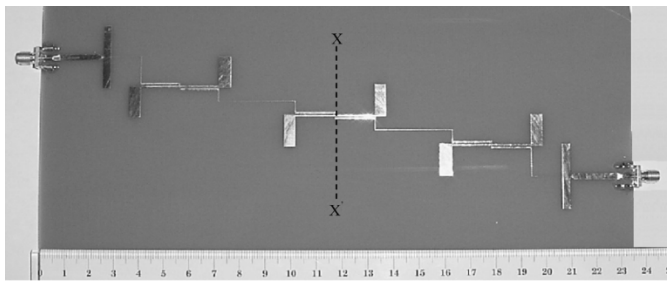

Fig. 7. PCB layout of the implemented filter.

For a seventh-order filter, there is only a pair of series short-circuited stubs left in the main line of the filter that must be approximated by high-impedance transmission lines. From Fig. 6(c), the scaled characteristic impedance L of one of these short-circuited stubs is (737.934/2.5) Ω. The highest characteristic impedance Z_o of a transmission that is realizable on our board is 137 Ω corresponding to a 7-mil-wide (0.177 mm) track. Thus, using (11), the quarter-wave-length frequency of the line is evaluated as follows:

$$f'_r = \frac{\pi}{2} \frac{137(1 \times 10^9)}{\left(\frac{737.934}{2.5}\right) \tan\left(\frac{\pi}{2} \frac{1}{2.75}\right)} = 1.134\ \text{GHz}. \tag{21}$$

At this stage, tuning of some of the element values of the filter is required to obtain a flat return loss over the passband. This leads to the electrical layout of the filter, as shown in Fig. 6(d). Examination of the inter-resonator couplings and stub impedances show that they can now be easily realized on our PCB. The electrical layout of filter was then converted into physical dimensions using ADS and the filter constructed. The overall length of the filter is 9449 mil (240 mm), as shown in Fig. 7.

V. Results and Discussion

The measured in-band performance of the constructed filter is shown in Fig. 8. The center frequency of the passband is offset by 65 MHz (6.5%), which could be compensated for by shortening the physical lengths of the transmission-line resonators. The midband insertion loss was 5.1 dB and the return loss was greater than 10 dB, as shown in Fig. 8(a). The simulated and measured wide-band scattering parameters of the filter from dc up to 10 GHz are illustrated in Fig. 8(b).

This filter was designed in Section IV to theoretically have its first pair of spurious passbands centered at 4.5 and 6.5 GHz should it be realized on a homogenous media. However, the simulated (dark) plot of Fig. 8(b) predicts that the first two spurious passbands are approximately centered at 5.25 and 7.25 GHz instead of 4.5 and 6.5 GHz. This difference is associated with the

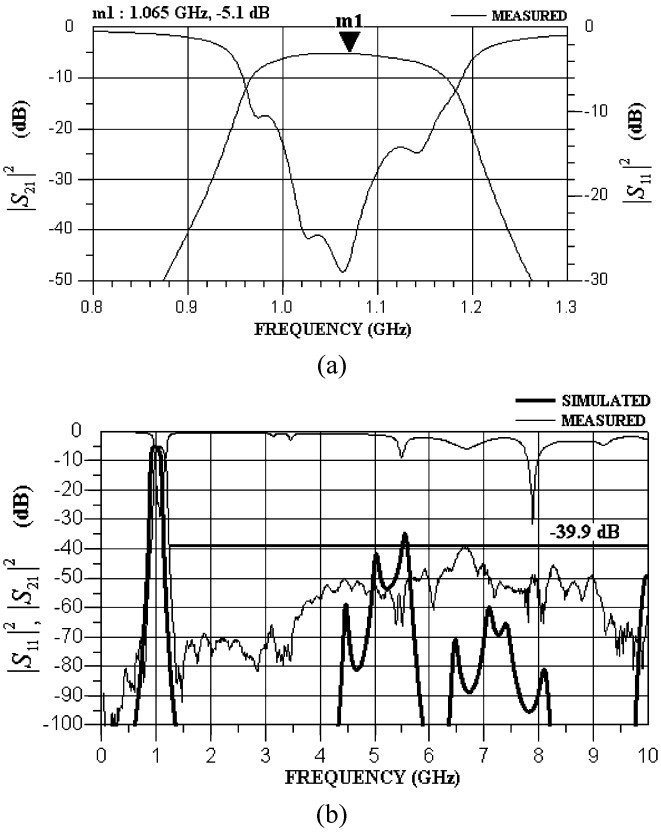

Fig. 8. Measured and simulated performances of the implemented PCL filter of Fig. 7. (a) In-band frequency response. (b) Wide-band frequency response.

inequality between the even- and odd-mode phase velocities of the microstrip media and also partially due to approximating the inner pair of short-circuited stubs in the f-plane filter by high-impedance transmission lines. In summary, the measured transmission performance of the filter followed the simulation and achieved an attenuation level exceeding 39.9 dB (i.e., an effective rejection level of approximately 35 dB) up to 10 GHz. As seen from Fig. 8(b), the stopband of the filter has a tendency to show a spurious passband at the region where the theoretical spurious passbands would have existed. This is around 6 GHz, as predicted by the simulation.

At this stage, the performance of the new PCL filter is compared with the characteristic of a conventional filter designed for the same fractional bandwidth, but of fifth order. The order of the filter was lowered to reduce the insertion loss level of its fundamental passband. The conventional filter has optimized stepped-impedance resonators [according to Fig. 2(a)] with the following parameters:

$$Z_s = 137\,\Omega \quad Z_r = 60\,\Omega \quad l_s = 325 \text{ mil } (8.25 \text{ mm}). \tag{22}$$

Its measured characteristic is shown in Fig. 9. As expected, a shift in the positions of the spurious passbands is observed, which complies with the argument presented in Section II and [16]. The measured midband insertion loss of the filter was 3.6 dB. Comparison of the stopband performances of the new and conventional filters highlights the improvements gained from the new design methodology.

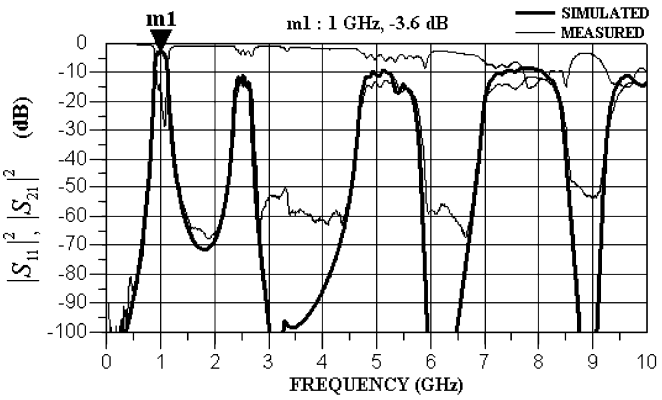

Fig. 9. Measured and simulated wide-band frequency responses of a conventional fifth-order PCL filter utilizing optimized (Type 1) stepped-impedance resonators [16].

VI. Conclusion

A circuit-oriented approach for the design of a new class of PCL filters has been presented in this paper. The PCL filters are driven from synthesized S-plane bandpass prototypes after appropriate circuit transformations. As a result, the filters have uniform- and stepped-impedance resonators, some of which are loaded by open-circuited stubs at their open-circuited ends. In comparison with the performances of conventional filters utilizing uniform- or stepped-impedance resonators, the new filters have broader stopband characteristics. This has been illustrated experimentally by the implementation of practical filters. It is believed that the new class of PCL filters will find wide usage in advanced RF/microwave front-end transceivers.

Appendix

The $ABCD$ matrix of a pair of uniform open-circuited coupled lines in an inhomogeneous media [27] is

$$A = \frac{Z_{oe}\cot(\theta_e) + Z_{oo}\cot(\theta_o)}{Z_{oe}\csc(\theta_e) - Z_{oo}\csc(\theta_o)} = D$$
$$B = \frac{j}{2}\frac{Z_{oe}^2 + Z_{oo}^2 - 2Z_{oe}Z_{oo}\big(\cot(\theta_e)\cot(\theta_o) + \csc(\theta_e)\csc(\theta_o)\big)}{Z_{oe}\csc(\theta_e) - Z_{oo}\csc(\theta_o)}$$
$$C = \frac{2j}{Z_{oe}\csc(\theta_e) - Z_{oo}\csc(\theta_o)} \tag{23}$$

where Z_{oe} and Z_{oo} are the modal impedances and θ_e and θ_o are the even- and odd-mode phase lengths.

References

[1] S. B. Cohn, "Parallel-coupled transmission-line resonator filters," *IRE Trans. Microw. Theory Tech.*, vol. MTT-6, no. 4, pp. 223–231, Apr. 1958.
[2] B. J. Minnis, "Printed circuit coupled-line filters for bandwidths up to and greater than an octave," *IEEE Trans. Microw. Theory Tech.*, vol. MTT-29, no. 3, pp. 215–222, Mar. 1981.
[3] I. Bahl, "Capacitively compensated high performance parallel coupled microstrip filters," in *IEEE MTT-S Int. Microwave Symp. Dig.*, Jun. 1989, pp. 679–682.
[4] S. M. Wang, C. H. Chi, M. Y. Hsieh, and C. Y. Chang, "Miniaturized spurious passband suppression microstrip filter using meandered parallel coupled lines," *IEEE Trans. Microw. Theory Tech.*, vol. 53, no. 2, pp. 747–753, Feb. 2005.
[5] M. C. Velazquez-Ahumada, J. Martel, and F. Medina, "Parallel coupled microstrip filters with ground-plane aperture for spurious band suppression and enhanced coupling," *IEEE Trans. Microw. Theory Tech.*, vol. 52, no. 3, pp. 1082–1086, Mar. 2004.

[6] ——, "Parallel coupled microstrip filters with floating ground-plane conductor for spurious-band suppression," *IEEE Trans. Microw. Theory Tech.*, vol. 53, no. 5, pp. 1823–1828, May 2005.
[7] L. Zhu, H. Bu, and K. Wu, "Broadband and compact multi-pole microstrip bandpass filters using ground plane aperture technique," *Proc. Inst. Elect. Eng.–Microwave Antennas Propag.*, vol. 149, pp. 71–77, Feb. 2002.
[8] J. T. Kuo, M. Jiang, and H. J. Chang, "Design of parallel-coupled microstrip filters with suppression of spurious resonances using substrate suspension," *IEEE Trans. Microw. Theory Tech.*, vol. 52, no. 1, pp. 83–89, Jan. 2004.
[9] J. T. Kuo and M. Jiang, "Enhanced microstrip filter design with a uniform dielectric overlay for suppressing the second harmonic response," *IEEE Microw. Wireless Compon. Lett.*, vol. 14, no. 9, pp. 419–421, Sep. 2004.
[10] T. Lopetegi, M. A. G. Laso, J. Hernandez, M. Bacaicoa, D. Benito, M. J. Garde, M. Sorolla, and M. Guglielmi, "New microstrip 'wiggly line' filters with spurious passband suppression," *IEEE Trans. Microw. Theory Tech.*, vol. 49, no. 9, pp. 1593–1598, Sep. 2001.
[11] T. Lopetegi, M. A. G. Laso, F. Falcone, F. Martin, J. Bonache, J. Garcia, L. Perz-Ceivas, M. Sorolla, and M. Guglielmi, "Microstrip 'wiggly line' filters with multispurious rejection," *IEEE Microw. Wireless Compon. Lett.*, vol. 14, no. 11, pp. 531–533, Nov. 2004.
[12] B. S. Kim, J. W. Lee, and M. S. Song, "An implementation of harmonic-suppression microstrip filters with periodic grooves," *IEEE Microw. Wireless Compon. Lett.*, vol. 14, no. 9, pp. 413–415, Sep. 2004.
[13] J. T. Kuo, W. H. Hsu, and W. T. Huang, "Parallel coupled microstrip filters with suppression of harmonic response," *IEEE Microw. Wireless Compon. Lett.*, vol. 12, no. 10, pp. 383–385, Oct. 2002.
[14] ——, "Tapped wiggly-coupled technique applied to microstrip bandpass filters for multi-octave spurious suppression," *Electron. Lett.*, vol. 40, pp. 46–47, Jan. 2004.
[15] J. Garcia-Garcia, F. Martin, F. Falcone, J. Bonache, I. Gil, T. Lopetegi, M. Laso, M. Sorolla, and R. Marques, "Spurious passband suppression in microstrip coupled line band pass filters by means of split ring resonators," *IEEE Microw. Wireless Compon. Lett.*, vol. 14, no. 9, pp. 416–418, Sep. 2004.
[16] M. Makimoto and S. Yamashita, "Bandpass filters using parallel coupled striplines stepped impedance resonators," *IEEE Trans. Microw. Theory Tech.*, vol. MTT-28, no. 12, pp. 1413–1417, Dec. 1980.
[17] P. Cheong, S. W. Fok, and K. W. Tam, "Miniaturized parallel coupled-line bandpass filter with spurious-response suppression," *IEEE Trans. Microw. Theory Tech.*, vol. 53, no. 5, pp. 1810–1816, May 2005.
[18] E. G. Cristal and S. Frankel, "Hairpin-line and hybrid hairpin-line/half-wave parallel-coupled-line filters," *IEEE Trans. Microw. Theory Tech.*, vol. MTT-20, no. 11, pp. 719–728, Nov. 1972.
[19] U. H. Gysel, "New theory and design for hairpin-line filters," *IEEE Trans. Microw. Theory Tech.*, vol. MTT-22, no. 5, pp. 523–531, May 1974.
[20] I. Hunter, *Theory and Design of Microwave Filters*. London, U.K.: IEE Press, 2001.
[21] G. Matthaei, L. Young, and E. M. T. Jones, *Microwave Filters, Impedance-Matching Networks, and Coupling Structures*. Norwood, MA: Artech House, 1980.
[22] M. Horton and R. Wenzel, "General theory and design of optimum quarter-wave TEM filters," *IEEE Trans. Microw. Theory Tech.*, vol. MTT-13, no. 5, pp. 316–327, May 1965.
[23] H. J. Orchard and G. C. Temes, "Filter design using transformed variable," *IEEE Trans. Circuit Theory*, vol. CT-15, no. 12, pp. 385–408, Dec. 1968.
[24] R. J. Wenzel, "Synthesis of combline and capacitively loaded interdigital bandpass filters of arbitrary bandwidth," *IEEE Trans. Microw. Theory Tech.*, vol. MTT-19, no. 8, pp. 678–686, Aug. 1971.
[25] J. A. G. Malherbe, *Microwave Transmission Line Filters*. Norwood, MA: Artech House, 1979.
[26] B. J. Minnis, *Designing Microwave Circuits by Exact Synthesis*. Norwood, MA: Artech House, 1996.
[27] G. I. Zysman and A. K. Johnson, "Coupled transmission line networks in an inhomogeneous dielectric medium," *IEEE Trans. Microw. Theory Tech.*, vol. MTT-17, no. 10, pp. 753–759, Oct. 1969.

Wael M. Fathelbab (M'03–SM'05) received the Bachelor of Engineering (B.Eng.) and Doctor of Philosophy (Ph.D.) degrees from the University of Bradford, Bradford, U.K., in 1995, and 1999 respectively.

From 1999 to 2001, he was an RF Engineer with Filtronic Comtek (U.K.) Ltd., where he was involved in the design and development of filters and multiplexers for various cellular base-station applications. He was subsequently involved with the design of novel RF front-end transceivers for the U.K. market with the Mobile Handset Division, NEC Technologies (U.K.) Ltd. He is currently a Research Associate with the Department of Electrical and Computer Engineering, North Carolina State University, Raleigh. His research interests include network filter theory, synthesis of passive and tunable microwave devices, and the design of broad-band matching circuits.

Michael B. Steer (S'76–M'82–SM'90–F'99) received the B.E. and Ph.D. degrees in electrical engineering from the University of Queensland, Brisbane, Australia, in 1976 and 1983, respectively.

He is currently a Professor with the Department of Electrical and Computer Engineering, North Carolina State University, Raleigh. In 1999 and 2000, he was a Professor with the School of Electronic and Electrical Engineering, The University of Leeds, where he held the Chair in microwave and millimeter-wave electronics. He was also Director of the Institute of Microwaves and Photonics, The University of Leeds. He has authored approximately 300 publications on topics related to RF, microwave and millimeter-wave systems, high-speed digital design, and RF and microwave design methodology and circuit simulation. He coauthored *Foundations of Interconnect and Microstrip Design* (New York: Wiley, 2000).

Prof. Steer is active in the IEEE Microwave Theory and Techniques Society (IEEE MTT-S). In 1997, he was secretary of the IEEE MTT-S. From 1998 to 2000, he was an elected member of its Administrative Committee. He is the Editor-in-Chief of the IEEE TRANSACTIONS ON MICROWAVE THEORY AND TECHNIQUES (2003–2006). He was a 1987 Presidential Young Investigator (USA). In 1994 and 1996, he was the recipient of the Bronze Medallion presented by the Army Research Office for "Outstanding Scientific Accomplishment." He was also the recipient of the 2003 Alcoa Foundation Distinguished Research Award presented by North Carolina State University.